



Temperature Dependence of the Pitch in Chiral Lyotropic Chromonic Liquid Crystals

Journal:	<i>Soft Matter</i>
Manuscript ID	SM-ART-10-2018-002091.R1
Article Type:	Paper
Date Submitted by the Author:	26-Nov-2018
Complete List of Authors:	Ogolla, Timothy; Kent State Univeristy, Chemical Physics Interdisciplinary Program Paley, Robert S.; Swarthmore College, Department of Chemistry & Biochemistry Collings, Peter; Swarthmore College, Physics & Astronomy

Cite this: DOI: 10.1039/xxxxxxxxxx

Temperature Dependence of the Pitch in Chiral Lyotropic Chromonic Liquid Crystals

Timothy Ogolla,^{‡,a,b} Robert S. Paley,^b and Peter J. Collings^{*,a,c}Received Date
Accepted Date

DOI: 10.1039/xxxxxxxxxx

www.rsc.org/journalname

One of the most simple cases in which chirality at the microscopic level produces a chiral macroscopic structure is the chiral nematic liquid crystal phase. In such a phase, the preferred direction of molecular orientation rotates in helical fashion, with the pitch of the helix in different systems ranging from around 100 nm to as large as can be measured (~10 mm). For almost all thermotropic and lyotropic liquid crystals, the ordered entities are formed from strong bonds, so the pitch varies in accordance with how the interactions between these largely immutable entities are affected by changing conditions. A unique exception are lyotropic chromonic liquid crystals (LCLCs) that spontaneously form weakly bound assemblies in solution, the size of which depends strongly on experimental parameters. While the temperature dependence of the pitch has been measured for chiral LCLCs formed by short strands of DNA (DNA-LCLCs), such is not the case for chiral LCLCs formed by small molecules. Polarized optical microscopy experiments on small molecule chiral LCLCs reveal the changing assembly size through a temperature dependence of the pitch not typical for many other systems, including the most recent measurements on DNA-LCLCs. In fact, the pitch measurements in small molecule chiral LCLCs strongly increase in value as the temperature is increased and the assemblies shrink in size. Theoretical considerations provide some help in understanding this phenomena, but leave much to be explained.

Introduction

Soft matter systems usually reveal the presence of chiral building blocks by organizing themselves into chiral structures. Liquid crystals are excellent examples of this, with the most simple case being the nematic phase in which the building blocks are orientationally but not positionally ordered. If the building blocks are chiral or if the system contains chiral dopants, the preferred direction of orientation adopts a macroscopic helix, revealing the presence of chirality at the microscopic level. The macroscopic helix is described by its pitch P , the distance over which the preferred direction rotates through 360° . This occurs in thermotropic liquid crystals, which are composed of individual molecules. It also happens in lyotropic liquid crystals, which are formed by a wide variety of viruses, macromolecules, or molecular assemblies in solution.

In thermotropic liquid crystals, if chiral dopant molecules are added to non-chiral liquid crystal molecules or if there is an enantiomeric excess of chiral liquid crystal molecules, the inverse pitch is proportional to the chiral dopant concentration or the enantiomeric excess. This simple relation is observed in many cases, (1) as long as the dopant concentration is not too large,¹ and (2) for all values of the enantiomeric excess.² The same is true for most lyotropic liquid crystals for the addition of chiral dopants in disk-like micelles³ and for the concentration of chiral rod-like viruses in solution.⁴ Exceptions to this rule, *i.e.*, nonlinear relationships between the inverse pitch and the concentration, often include cases in which a helix inversion point or a transition to a smectic phase is nearby. This behavior is best revealed by the the strong increase of the pitch as the helix inversion point or smectic transition is approached.⁵ Otherwise, the pitch only weakly depends on the temperature, with the general trend being that the pitch decreases with increasing temperature.^{3,5}

One important aspect of the systems under discussion is that the ordering entities, the molecules in the case of thermotropic liquid crystals and the macromolecules or molecular assemblies in the case of lyotropic liquid crystals, are bonded together strongly enough that the size of the ordering entity does not change as the temperature is varied. This is absolutely true for thermotropic liquid crystals, and is approximately true for most lyotropic liquid

^a Department of Physics & Astronomy, Swarthmore College, Swarthmore, PA, U.S.A. Fax: 610 328 7895; Tel: 610 328 7791; E-mail: pcollin1@swarthmore.edu

^b Department of Chemistry and Biochemistry, Swarthmore College, Swarthmore, PA, U.S.A.

^c Department of Physics and Astronomy, University of Pennsylvania, Philadelphia, PA, U.S.A.

* Corresponding Author.

[‡] Present Address: Chemical Physics Interdisciplinary Program, Kent State University, Kent, OH, U.S.A.

crystals for changes in temperature that are not too large. Hence the change in the pitch due to a change in concentration of the chiral component or a change in temperature reflects how the chiral interactions between the more or less unchanging ordering entities are affected. Since the pitch is determined by the competition between Frank elastic energy terms that resist and favor twist deformation, the general decrease in the pitch as the temperature is increased, for example, reflects the fact that the elastic energy terms resisting twist decrease faster than those favoring twist. Two exceptions to this general trend are the thermotropic liquid crystal CEEC⁶ and suspensions of the rod-like filamentous bacteriophage *fd*,⁷ which show an increasing pitch with increasing temperature.

On the other hand, if the size of the ordering entities depends on temperature strongly enough, then the elastic energy terms may behave differently relative to each other. This is the case for lyotropic chromonic liquid crystals (LCLCs), in which molecules in solution spontaneously form weakly bound anisotropic assemblies that orientationally order at high enough concentrations.⁸ LCLCs typically form from aqueous solutions of certain plank-shaped molecules with aromatic cores and polar groups on the peripheries. Many dyes and drugs form LCLCs, but short oligimers of nucleic acids (DNA-LCLCs) also behave similarly. The molecules or oligimers in LCLCs tend to stack face-to-face, forming rod-like assemblies that order into a nematic or columnar liquid crystal phase. In equilibrium, the length distribution is statistical and thus extremely broad. As the temperature is increased, the length distribution shifts to shorter assemblies, decreasing the concentration of the longer assemblies and increasing the concentration of the shorter ones. This change in the distribution of assembly size affects the elastic energy terms resisting and favoring twist in a way not possible in thermotropic and most lyotropic liquid crystals. If the elastic energy terms promoting twist decrease faster than the terms resisting twist, the pitch increases with increasing temperature, which is opposite to what is encountered in most thermotropic and lyotropic liquid crystals.

Studies of LCLCs have increased in importance over the last decade because they are aqueous solutions and therefore relevant to biology and medicine. Although a couple of experiments were done on small molecule chiral LCLCs over 30 years ago,^{9,10} such investigations have increased in number more recently, both with systems composed of small molecule non-chiral LCLCs and chiral dopants,^{11–14} and with small molecule chiral LCLCs.^{11,15–17} Interest in DNA-LCLCs, in which the short oligimers of DNA are chiral, has also increased recently.^{18,19} This report describes experiments measuring the temperature dependence of the pitch for the small molecule non-chiral LCLC disodium cromoglycate (DSCG) doped with various chiral molecules. In all cases, an increase in the pitch with increasing temperature is observed, although the temperature range over which this occurs (just below the transition to the chiral nematic - isotropic coexistence region) varies considerably. In the latest measurement on DNA-LCLCs,¹⁹ the pitch decreases as the temperature increases toward the biphasic region, although in an earlier experiment, the pitch increased with increasing temperature for most of the DNA-LCLCs investigated.¹⁸ In addition, one experiment on an LCLC composed of

small chiral molecules is reported here and shows that it behaves similarly to the doped systems. Certain theoretical ideas suggest that the pitch increases with temperature if achiral hard-core repulsion dominates the chiral attractive interactions,²⁰ which is consistent with the data within 8 K of the boundary with the chiral nematic - isotropic coexistence region. However, this is just one of many theoretical results, most of which apply to chiral entities as opposed to chiral dopants. Nonetheless, the experimental results reported here demonstrate an important difference between small molecule LCLCs and thermotropic and most lyotropic liquid crystals, and even some DNA-LCLCs.

Theory

LCLC Assemblies.

Several comprehensive reviews of LCLCs have appeared recently.^{8,21} Perhaps the most unique property of LCLCs is that the size distribution of the assemblies is very sensitive to properties such as concentration and temperature. The most simple model for the assembly process assumes that the free energy change for a molecule to join an assembly is independent of the size of the assembly. This isodesmic assembly process has been examined both by computer simulation²² and experimental investigation,²³ with the finding that the isodesmic assumption is not followed exactly, but is close to being true and therefore quite useful due to its simplicity.

If the equilibrium constant for a molecule to join an aggregate is denoted by K , the concentration of single molecules ρ_1 and the concentration of assemblies with i molecules ρ_i can be calculated from

$$\rho_1 = \frac{2K\rho_T + 1 - \sqrt{4K\rho_T + 1}}{2K^2\rho_T},$$

$$\rho_i = K^{i-1}\rho_1^i, \quad (1)$$

where $K = \exp \frac{\Delta G T_0}{T}$.

ρ_T is the total concentration of molecules, T is the temperature, and ΔG is the free energy change at temperature T_0 for a molecule to join an aggregate (in units of $k_B T_0$, where k_B is the Boltzmann constant).²¹ Notice that the concentration of assemblies of different sizes is a decreasing exponential function of the size i . Changing the temperature simply changes the characteristic size of the exponential distribution, $-1/\ln(K\rho_1)$. Of interest is the average number of molecules in an assembly. This is given by

$$\langle i \rangle = \frac{\sum_{i=1}^{\infty} i\rho_i}{\sum_{i=1}^{\infty} \rho_i} = \frac{1}{1 - K\rho_1}. \quad (2)$$

So for example, if $\Delta G = 7 k_B T$ and $T_0 = 295$ K, the average number of molecules in assemblies ranges from 14.8 at 288 K to 12.6 at 303 K, a change of 15% over this 15 K range.

While the isodesmic assumption produces a model for the assembly process, more is necessary in order to understand the origin of the liquid crystal phases. Early work added a scaled

particle calculation of the configurational entropy of hard-rods together with a short-range repulsive potential to ensure system stability.^{24,25} More recent theoretical investigations tend to rely on computer simulation.^{22,26–30} This work has helped to provide insight into both the structure of the assemblies and the nematic/columnar phases they form.

Chiral Nematic Pitch.

The free energy associated with distortion of the director of a chiral nematic liquid crystal is given by the Frank free energy, with the energy per unit volume f_V given by

$$f_V = -k_2(\hat{n} \cdot \nabla \times \hat{n}) + \frac{1}{2}k_{11}(\nabla \cdot \hat{n})^2 + \frac{1}{2}k_{22}(\hat{n} \cdot \nabla \times \hat{n})^2 + \frac{1}{2}k_{33}|\hat{n} \times (\nabla \times \hat{n})|^2, \quad (3)$$

where \hat{n} is the liquid crystal director, k_{11} , k_{22} , and k_{33} are the splay, twist, and bend elastic constants, respectively, and k_2 is the parameter related to the chirality of the liquid crystal.³¹ The chirality of the liquid crystal is given by q_0 , which is equal to k_2/k_{22} . The pitch P is related to the chirality by $q_0 = 2\pi/P$.

The literature discussing the theory of chiral nematic ordering is extensive, but a few examples are included here in anticipation of the experimental results. The seminal work of Straley^{32,33} involved a statistical mechanical theory of threaded rods based on the Onsager expansion. L is the length of the rod, D is the diameter of the rod, and Δ is the thickness of the thread added to the rod of diameter D . Proportionalities for $|k_2|$ and k_{22} according to this theory are,

$$|k_2| \sim \rho^2 L^2 D \Delta S^2 k_B T$$

$$k_{22} \sim \rho^2 L^4 D k_B T, \quad (4)$$

where ρ is the number density of the rods and S is the orientational order parameter. Osipov³⁴ considered a molecular statistical model for the chiral nematic phase of chiral macromolecules in a solvent and of non-chiral molecules in a solvent of chiral molecules. By including chiral dispersion interactions and steric repulsions, expressions similar to Eq. (4) result, but k_2 can be positive or negative depending on the relative strength of the dispersion and steric interactions. This result therefore predicts the possibility of a helix inversion for chiral macromolecule solutions, which has been seen experimentally. Later a generalized van der Waals theory was developed, with the interesting result that q_0 is proportional to the volume fraction of rods and proportional to the length of the rods if the aspect ratio of the rods, number density, and temperature are fixed.²⁰ An Onsager-like theory by Frezza *et al.*³⁵ demonstrated that the relationship between the morphology of hard helical particles (handedness and curliness) and the pitch and handedness of the chiral nematic phase is quite complex. These predictions were supported by Monte Carlo simulations of the isotropic phase. Later, Dussi *et al.*³⁶ showed with classical density functional theory and Monte Carlo calculations that the handedness of the phase depends on a subtle combination of particle geometry and system density. In work aimed at DNA-LCLCs, Michelle *et al.*¹⁹ utilized a classical density functional theory that assumes steric repulsions are dominant to

connect the macroscopic pitch to structural features of the DNA oligomers. The prediction of an decreasing pitch with increasing temperature agreed with the most recent data. Finally, Ruzicka and Wensink³⁷ conducted a simulation of rods with patchy spheres arranged along a spiral on the rod surface. The spheres interact with each other via a Weeks-Chandler-Anderson potential and a repulsive Yukawa potential. The chirality q_0 depends on the volume fraction, the pitch of the patchy spheres, and the amplitude of the interactions. The simulation allows for a helix inversion and q_0 once again is proportional to the volume fraction.

Experimental Procedures

All the amino acids (*l*-alanine, *l*-arginine hydrochloride, *d*-lysine hydrochloride, and *trans*-4-hydroxy-*l*-proline) and DSCG were purchased from Sigma-Aldrich and used without further purification. (S)-(-)-2-aminomethyl-1-ethylpyrrolidine 3,4,9,10-perylenebis(dicarboximide) (chiral-PDI) was synthesized using a modified procedure to that presented by Naidu *et al.*³⁸ and Kularatne *et al.*¹⁶. Perylene-3,4,9,10-tetracarboxylic dianhydride and (S)-(-)-2-aminomethyl-1-ethylpyrrolidine were dissolved in dimethyl formamide in a round bottomed flask and stirred at 70°C for 24 hours. After cooling, the reaction mixture was filtered, and the recovered solid was washed with methanol and ethyl acetate. The product was dried under vacuum to obtain chiral-PDI with 94% yield. A proton NMR spectrum was taken in deuterated chloroform to verify the identity of the product. All DSCG mixtures were made with solutions of an amino acid in Millipore water. In order to form the chiral-PDI salt, mixtures of chiral-PDI were made with stoichiometric concentrations of reagent grade hydrochloric acid in Millipore water.

The final mixtures were stirred and heated at 60°C until all the solid dissolved. The same stirring and heating was performed for roughly a half hour before loading the mixture into rectangular or square capillaries by capillary action at 60°C. The thickness of the rectangular capillaries ranged from 100 to 400 μm . The dimension of the square capillaries was 0.5 or 1.0 mm. Immediately after filling, the capillary was sealed by epoxy and fixed to a microscope slide.

The pitch measurements were done using polarizing optical microscopy (POM) with the sample between two linear polarizers as described by Ogolla *et al.*¹³. The angle between the polarizers and the orientation of the sample were adjusted to optimize the brightness and contrast in different regions of the sample. For the amino acid mixtures, the microscope (Leitz Laborlux 12 Pol) was equipped with a camera (Zeiss AxioCam ICc 1). Images were taken using ZEN software with either 10X or 25X objectives. A region of interest was specified and an intensity profile generated perpendicular to the parallel striations of the fingerprint texture. The pitch was determined by measuring the average distance between the striations and multiplying by two. The temperature of the sample was controlled by an Instec HC5302 heating stage. For the chiral-PDI sample, a Zeiss Axio Imager 2 microscope with a 50X objective and ZEN software was used with a Linkum LTS420 hot stage.

The sample was allowed to equilibrate for at least 45 minutes

at the lowest temperature before starting pitch measurements. At each temperature, the sample equilibrated for at least 8 minutes before measuring the pitch. When the pitch was large, often the planar texture was present instead of the fingerprint texture. Because the fingerprint texture was still observed for long pitches in square capillaries, these were used when necessary. In this way, pitch measurements were performed as the temperature approached the chiral nematic - isotropic coexistence region and the pitch became large. Measurements were made for all temperatures up to and including T_C , the temperature at which droplets of the isotropic phase first appeared.

Experimental Results

The temperature dependent pitch measurements are shown in Fig. 1 for 16 wt% DSCG in seven amino acid solutions. As reported in Ogolla *et al.*¹³, T_C is not sensitive to the chiral dopant concentration except for *l*-arginine hydrochloride (see Table 1). Notice that for all mixtures, the pitch tends to increase as T_C is approached, for some quite modestly, but for most quite dramatically. Notice also that for mixtures with a larger pitch, the pitch increases monotonically as T_C is approached. When the pitch is smaller, the pitch decreases with temperature before increasing with temperature close to T_C .

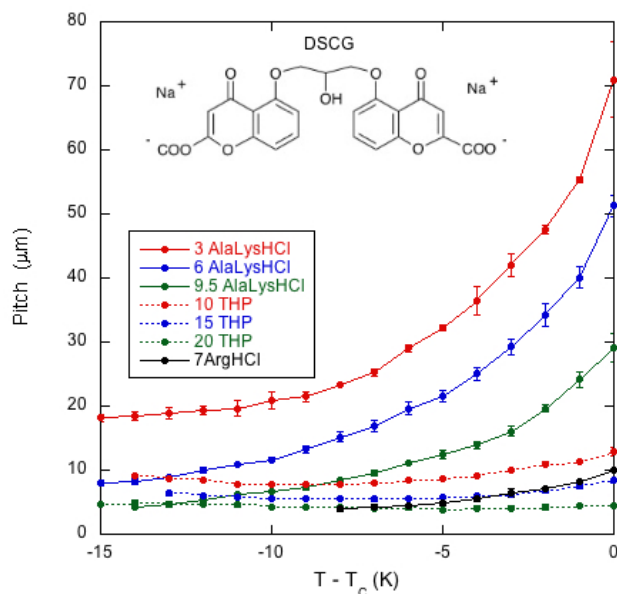


Fig. 1 Temperature dependence of the pitch in the chiral nematic phase of 16 wt% DSCG (structure shown) in seven amino acid solutions: 3, 6, and 9.5 wt% of both *l*-alanine and *d*-lysine hydrochloride (AlaLysHCl), 10, 15, and 20 wt% of *trans*-4-hydroxy-*l*-proline (THP), and 7 wt% of *l*-arginine hydrochloride (ArgHCl). T_C is the temperature of the boundary between the chiral nematic phase and the chiral nematic - isotropic coexistence region and is given in Table 1. The helix in the chiral nematic phase is right-handed for all solutions except ArgHCl which is left-handed.^{9,10}

To make the connection with theory more apparent, the chirality $q_0 = 2\pi/P$ is plotted versus temperature in Fig. 2. Notice that the chirality decreases dramatically as T_C is approached for all mixtures except for DSCG in a 20 wt% solution of *trans*-4-

Table 1 Transition temperatures from the chiral nematic phase to the chiral nematic - isotropic coexistence region. Equal concentrations of *l*-alanine and *d*-lysine HCl are used for three of the samples, and the concentration of each is given in the table.

Dopant	Concentration	Temperature (°C)
none	0.0	31
<i>l</i> -alanine & <i>d</i> -lysine HCl	3.0	31
<i>l</i> -alanine & <i>d</i> -lysine HCl	6.0	31
<i>l</i> -alanine & <i>d</i> -lysine HCl	9.5	30
<i>trans</i> -4-hydroxy- <i>l</i> -proline	10.0	30
<i>trans</i> -4-hydroxy- <i>l</i> -proline	15.0	31
<i>trans</i> -4-hydroxy- <i>l</i> -proline	20.0	30
<i>l</i> -arginine HCl	7.0	24

hydroxy-*l*-proline. The minimum of the pitch (maximum in q_0) is quite evident for the *trans*-4-hydroxy-*l*-proline mixtures.

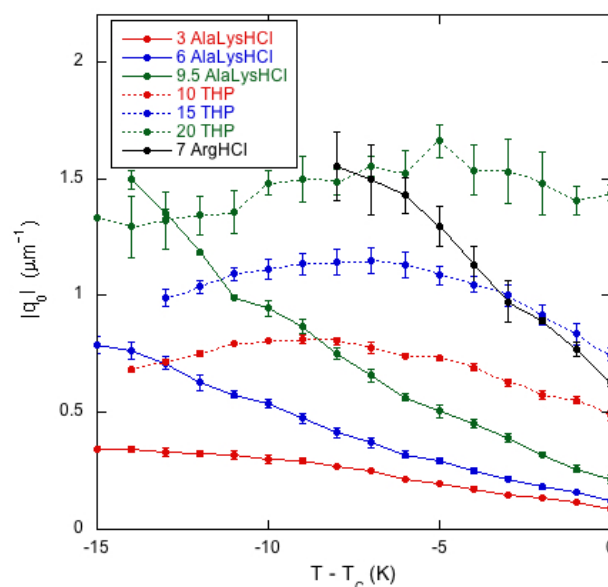


Fig. 2 Temperature dependence in the chiral nematic phase of the chirality $q_0 = 2\pi/P$ for 16 wt% DSCG in seven solutions of amino acids. The labels are the same as in Fig. 1. T_C is the temperature of the boundary between the chiral nematic phase and the chiral nematic - isotropic coexistence region and is given in Table 1.

In order to compare chiral doped LCLCs with chiral LCLCs, the investigation included a single experiment on chiral-PDI. The pitch of 12 wt% chiral-PDI is quite short,^{15,16} necessitating the need for the more powerful microscope. Even over the wider temperature range investigated, as shown in Fig. 3, the pitch increases and the chirality decreases in much the same way as the shorter pitch mixtures of DSCG in amino acid solutions.

Discussion

The results clearly demonstrate that the pitch increases (and the chirality decreases) near the transition to the chiral nematic - isotropic coexistence region for all the chiral dopants. This is important for the specific case of *l*-arginine hydrochloride. In an investigation of the helical twisting power of DSCG in various amino acid solutions,¹³ the helical twisting power increases linearly with chiral dopant concentration for low concentrations of

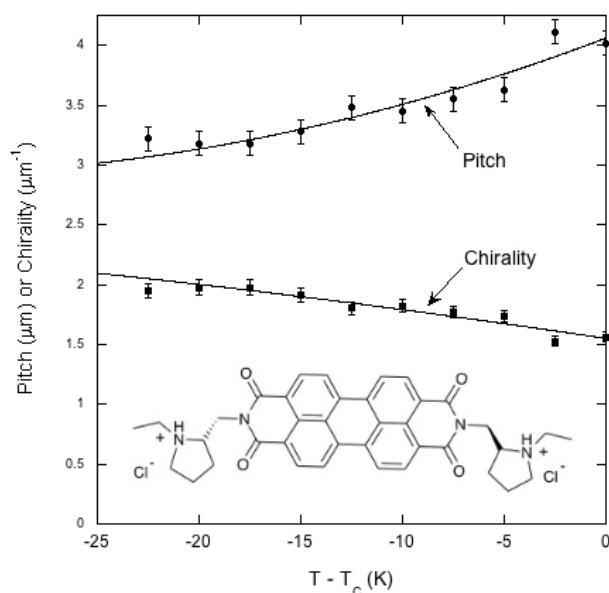


Fig. 3 Temperature dependence of the pitch and chirality for 12 wt% chiral-PDI (structure shown) in the chiral nematic phase. The handedness of the helix in the chiral nematic phase has not been measured. T_C is the temperature of the boundary between the chiral nematic phase and the chiral nematic - isotropic coexistence region and is equal to 50°C. The lines are drawn to aid the eye.

all the amino acids. Whereas many show slight non-linearity at higher concentrations, one amino acid, *l*-arginine hydrochloride, displays such a nonlinear behavior that it reaches a maximum value of the helical twisting power and decreases as the concentration is increased more. A hint as to the cause of this behavior comes from the fact that the temperature of the transition to the coexistence region decreases as the chiral dopant concentration is increased much more rapidly for *l*-arginine hydrochloride than all the other chiral dopants investigated. Thus as the *l*-arginine hydrochloride concentration increases, the measurements at room temperature take place closer and closer to the transition. If the pitch increases as the transition is approached, then the helical twisting power decreases if the pitch is more sensitive to temperature than to concentration. The results presented here for *l*-arginine hydrochloride confirm this conjecture and allow for a firm conclusion as to the cause of the extreme nonlinearity of the helical twisting power data.

Although DSCG with chiral dopants has not been the subject of many investigations, pure DSCG has been extensively investigated. For example, the twist elastic constant k_{22} has been measured for DSCG,³⁹ so one must ask whether the data on DSCG can be used to analyze the data on DSCG with chiral dopants. As evident from Fig. 4, the k_{22} data for DSCG show a linear temperature dependence for all concentrations. Notice that the value of k_{22} at T_C is weakly dependent on the DSCG concentration, while the linear dependence on $T - T_C$ is stronger. The difference between the doped and pure 16 wt% DSCG solutions is that in the doped samples 3 to 20 wt% is a chiral compound instead of water. Since the shift in T_C is less than 1 K for all dopants except arginine hydrochloride (see Table 1), in all likelihood k_{22} for those doped

samples is similar to the pure 16 wt% data in Fig. 4. Supporting evidence for this assertion is the general finding that adding various compounds to DSCG usually does little more than change T_C .^{40–42} Additionally, measurements in another small molecule LCLC, Sunset Yellow FCF, reveal a almost universal function between the order parameter and temperature if S is plotted against $T - T_C$.⁴³ Since $|q_0| = |k_2|/k_{22}$, using the $|q_0|$ data of Fig. 2 and the k_{22} data for 16 wt% DSCG from Fig. 4, namely k_{22} (in pN) = $0.410 - 0.0674(T - T_C)$ with $T - T_C$ in K, one can determine the temperature dependence of the chirality parameter $|k_2|$ for all the doped systems. This is shown in Fig. 5, where it is clear that $|k_2|$ for all dopants strongly decreases as T_C is approached. Note that $|k_2|$ decreases monotonically for the three THP solutions, even though P and $|q_0|$ show non-monotonic temperature dependences. While using the k_{22} data for pure DSCG brings some uncertainty to the calculated $|k_2|$ results, the strong decrease in $|k_2|$ is a robust qualitative finding. After all, both $|q_0|$ and k_{22} decrease as the temperature increases. Since $|k_2|$ depends on the product of these two quantities, it must decrease more rapidly.

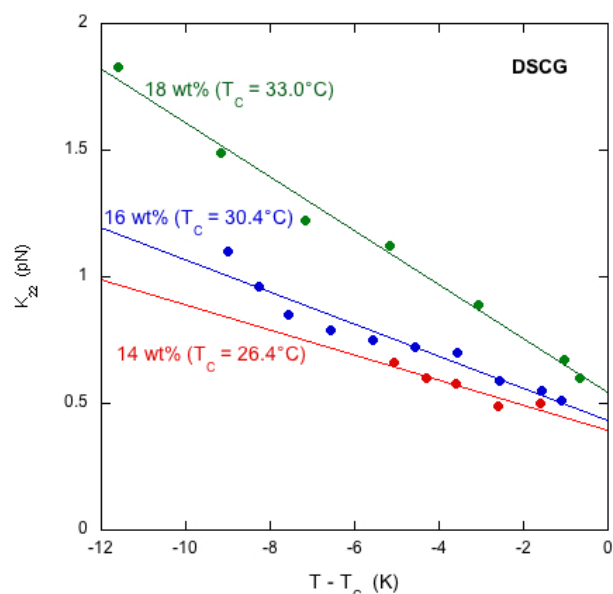


Fig. 4 Temperature dependence the twist elastic constant k_{22} for three concentrations of DSCG (taken from Zhou *et al.*³⁹). T_C is the temperature of the transition from the chiral nematic phase to the chiral nematic - isotropic coexistence region. The lines are least-squares linear fits to the data.

As an addendum, it is interesting to note that simple theoretical predictions are qualitatively consistent with the experimental data. According to Eq. (4), $|k_2|$ should be proportional to $\rho^2 L^2 S^2 T$. The number density of assemblies ρ in a LCLC is not well defined because of the wide distribution in assembly size. However, an estimate can be obtained by dividing the total DSCG concentration by the average number of molecules in an assembly $\langle i \rangle$, calculated from Eq. (2) with ΔG equal to $7 k_B T$.^{44,45} But if $\langle i \rangle$ is used as a quantity proportional to the average length of the assemblies, then ρL does not depend on $\langle i \rangle$. There have been some temperature-dependent measurements of the order parameter in DSCG, but they are not complete enough for an analysis. It is

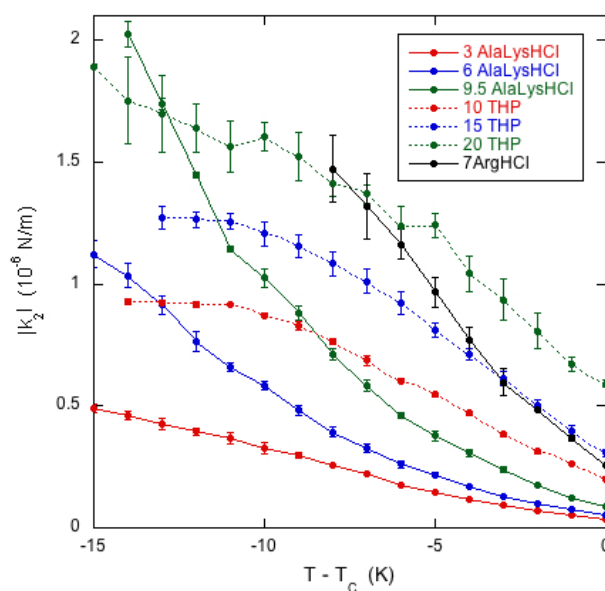


Fig. 5 Temperature dependence in the chiral parameter $|k_2|$ for 16 wt% DSCG in seven solutions of amino acids. The labels are the same as in Fig. 1. T_C is the temperature of the boundary between the chiral nematic phase and the chiral nematic - isotropic coexistence region and is given in Table 1.

better to assume that the order parameter is proportional to the birefringence, as is true for the LCLC Sunset Yellow FCF,⁴⁶ and use the high quality data on the birefringence of DSCG in place of the order parameter.⁴⁷ This analysis is made more simple by fitting the Haller approximation for the birefringence Δn to the DSCG data,

$$\Delta n = \Delta n_0 \left(1 - \frac{T}{T_C}\right)^\beta, \quad (5)$$

where T_C is the transition temperature to the chiral nematic - isotropic coexistence region, and Δn_0 and β are fitting constants (equal to -0.034 ± 0.001 and 0.20 ± 0.01 , respectively, for 16 wt% DSCG). Therefore, assuming ρL is constant with temperature, and $\langle i \rangle$ and $|\Delta n|$ are proportional to L and S , respectively, Eq. (4) can be utilized to plot the variation of $|k_2|$, k_{22} , and $|q_0| = |k_2|/k_{22}$ versus temperature. The results are shown in Fig. 6, where $|k_2|$ clearly decreases near the transition. Notice that k_{22} decreases less strongly, meaning that $|q_0|$ decreases also in the vicinity of T_C . The general trends exhibited in Fig. 6 are not unlike the data shown in Figs. 2, 4, and 5.

Michelle *et al.*¹⁹ make a different prediction in their theory of DNA oligomers. While k_{22} decreases with increasing temperature near the transition, $|k_2|$ increases. This means that $|q_0|$ increases with temperature, which is in agreement with the most recent experimental data on short DNA oligomers. The difference between the two theoretical predictions can be traced back to the dependence of $|k_2|$ on the length of the assemblies. Whereas by Eq. (4) $|k_2|$ increases with L if other parameters remain constant, in Ref. 19, $|k_2|$ decreases with the number of monomers in the assembly. This situation is highlighted in the theory of Dussi *et al.*³⁶ For certain choices of particle shape, increasing the length of the particle drives q_0 through zero. This means that $|k_2|$ can both de-

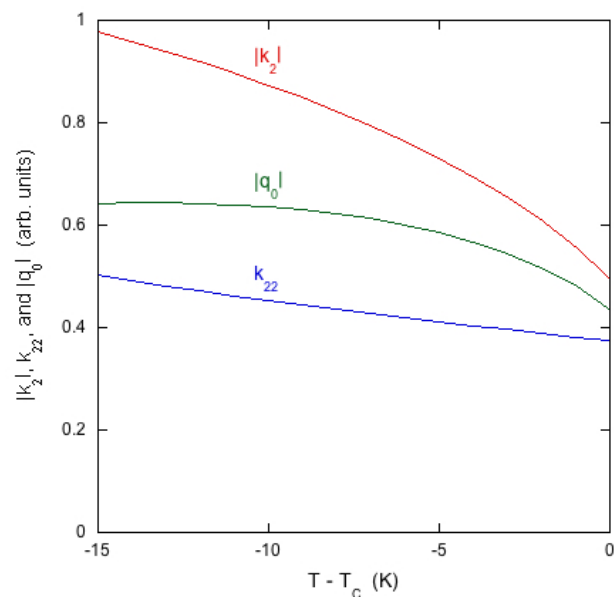


Fig. 6 Predictions of Eq. (4) for the chiral DSCG system as explained in the text. The vertical scale for each quantity is arbitrary except that the zero for each scale is the same.

crease and increase with increasing particle length depending on the detailed shape of the particle, which may explain why both increasing and decreasing $|q_0|$ trends were observed by Zanchetta *et al.*¹⁸ for various short DNA oligomers.

Conclusions

Lyotropic chromonic liquid crystals are a unique ordered fluid because the distribution of assembly size depends on concentration and temperature. The results presented here for small molecule LCLCs reveal this uniqueness in the temperature dependence of the pitch in the chiral nematic phase near the transition to the chiral nematic - isotropic coexistence region. This result appears to be quite robust, in that similar behavior is observed in small molecule systems with non-chiral LCLC molecules and chiral dopants and with chiral LCLC molecules. With both similar and opposite behavior having been observed in short oligomers of DNA, and with a good number of theories predicting the possibility of a helix inversion, which might explain why both types of behavior are observed, a full understanding can only come from additional theoretical and experimental research on LCLC systems.

Conflicts of interest

The authors declare no conflicts of interest.

Acknowledgements

This work was partially supported by the National Science Foundation through the University of Pennsylvania Materials Research Science and Engineering Center (MRSEC), Grant Nos. DMR11-20901 and DMR17-20530. T. O. acknowledges summer research support from Swarthmore College. All authors thank Sophie Ettinger for help with the more powerful microscope and Angel Martinez and Alexis de la Cotte for useful discussions.

Notes and references

- 1 F. Castles and S. Morris, *Handbook of Liquid Crystals*, Wiley-VCH, Weinheim, Germany, 2014, vol. 3, ch. 15, pp. 493–520.
- 2 D. K. Yang and P. P. Crooker, *Physical Review A*, 1987, **35**, 4419–4423.
- 3 K. Hiltrop, *Chirality in Liquid Crystals*, Springer-Verlag, New York, 2001, ch. 14, pp. 447–480.
- 4 E. Grelet and S. Fraden, *Physical Review Letters*, 2003, **90**, 198302–1 – 4.
- 5 I. Dierking, *Symmetry*, 2014, **6**, 444–472.
- 6 T. Harada and P. Crooker, *Mol. Cryst. Liq. Cryst.*, 1975, **30**, 79–86.
- 7 Z. Dogic and S. Fraden, *Langmuir*, 2000, **16**, 7820–7824.
- 8 J. Lydon, *Handbook of Liquid Crystals*, Wiley-VCH, Weinheim, Germany, 2014, vol. 6, ch. 14, pp. 439–483.
- 9 H. Lee and M. M. Labes, *Mol. Cryst. Liq. Cryst.*, 1982, **84**, 137–157.
- 10 H. Lee and M. M. Labes, *Mol. Cryst. Liq. Cryst.*, 1984, **108**, 125–132.
- 11 S. Yang, B. Wang, D. Cui, D. Kerwood, S. Wilkens, J. Han and Y. Y. Luk, *J. Phys. Chem. B*, 2013, **117**, 7133–7143.
- 12 C. Peng and O. D. Lavrentovich, *Soft Matter*, 2015, **11**, 7257–7263.
- 13 T. Ogolla, S. B. Nashed and P. J. Collings, *Liquid Crystals*, 2017, **44**, 1968–1978.
- 14 T. Shirai, M. Shuai, K. Nakamura, A. Yamaguchi, Y. Naka, T. Sasaki, N. A. Clark and K. V. Le, *Soft Matter*, 2018, **14**, 1511–1516.
- 15 L. P. Joshi, *PhD thesis*, Kent State University, 2009.
- 16 R. Kularatne, H. Kim, M. Ammanamanchi, H. N. Hayenga and T. H. Ware, *Chem. Mater.*, 2016, **28**, 8489–8492.
- 17 F. Berride, E. Troche-Pesqueira, G. Feio, E. J. Cabrita, T. Sierra, A. Navarro-Vazquez and M. M. Cid, *Soft Matter*, 2017, **13**, 6810–6815.
- 18 G. Zanchetta, F. Giavazzi, M. Nakata, M. Buscaglia, R. Cerbino, N. A. Clark and T. Bellini, *Proc. Nat. Acad. Sci.*, 2010, **107**, 617497–17502.
- 19 C. D. Michelle, G. Zanchetta, T. Bellini, E. Frezza and A. Ferrarini, *ACS Macro Lett.*, 2016, **5**, 208–212.
- 20 H. H. Wensink and G. Jackson, *J. Chem. Phys.*, 2009, **130**, 234911–1 – 234911–15.
- 21 P. J. Collings, J. N. Goldstein, E. J. Hamilton, B. R. Mercado, K. J. Nieser and M. H. Regan, *Liquid Crystal Reviews*, 2015, **3**, 1–27.
- 22 F. Chami and M. R. Wilson, *J. Am. Chem. Soc.*, 2010, **132**, 7794–7802.
- 23 L. Joshi, S. W. Kang, D. M. Agra-Kooijman and S. Kumar, *Phys. Rev. E*, 2009, **80**, 041703–1 – 041703–8.
- 24 M. P. Taylor and J. Herzfeld, *Langmuir*, 1990, **6**, 911–915.
- 25 M. P. Taylor and J. Herzfeld, *Phys. Rev. A*, 1991, **43**, 1892–1905.
- 26 P. K. Maiti, Y. Lansac, M. A. Glazer and N. A. Clark, *Liq. Cryst.*, 2002, **29**, 619–626.
- 27 T. Kuriabova, M. D. Betterton and M. A. Glaser, *J. Mater. Chem.*, 2010, **20**, 10366–10383.
- 28 M. Walker, A. J. Masters and M. R. Wilson, *Phys. Chem. Chem. Phys.*, 2014, **16**, 23074–23081.
- 29 A. Akinshina, M. Walker, M. R. Wilson, G. J. T. Tiddy, A. J. Masters and P. Carbone, *Soft Matter*, 2015, **11**, 680–691.
- 30 H. Sidky and J. K. Whitmer, *J. Phys. Chem. B*, 2018, **121**, 6691–6698.
- 31 L. M. Blinov, *Structure and Properties of Liquid Crystals*, Springer, Heidelberg, 2012, pp. 199–205, 274–275.
- 32 J. P. Straley, *Phys. Rev. A*, 1973, **8**, 2181–2183.
- 33 J. P. Straley, *Phys. Rev. A*, 1976, **14**, 1835–1841.
- 34 M. A. Osipov, *Il Nuovo Cimento*, 1988, **10**, 1249–1262.
- 35 E. Frezza, A. Ferrarini, H. B. Kolli, A. Giacometti and G. Cinacchi, *Phys. Chem. Chem. Phys.*, 2014, **16**, 16225–16232.
- 36 S. Dussi, S. Belli, R. van Roij and M. Dijkstra, *J. Chem. Phys.*, 2015, **142**, 074905–1 – 074905–16.
- 37 S. Ruzicka and H. H. Wensink, *Soft Matter*, 2016, **12**, 5205–5213.
- 38 J. J. Naidu, Y. J. Bae, K. U. Jeong, S. H. Lee, S. Kang and M. H. Lee, *Bull. Korean Chem. Soc.*, 2009, **30**, 935–937.
- 39 S. Zhou, K. Neupane, Y. A. Nastishin, A. R. Baldwin, S. V. Shiyonovskii, O. D. Lavrentovich and S. Sprunt, *Soft Matter*, 2014, **10**, 6571–6581.
- 40 L. Tortora, H. S. Park, K. Antion, D. Finotello and O. D. Lavrentovich, *Proc. of SPIE*, 2007, **6487**, 64870I–1 – 64870I–15.
- 41 L. Tortora, H. S. Park, S. W. Kang, V. Savaryn, S. H. Hong, K. Kaznatcheev, D. Finotello, S. Sprunt, S. Kumar and O. D. Lavrentovich, *Soft Matter*, 2010, **6**, 4157–4167.
- 42 H. S. Park, S. W. Kang, L. Tortora, S. Kumar and O. D. Lavrentovich, *Langmuir*, 2011, **27**, 4164–4175.
- 43 K. Nayani, J. Fu, R. Chang, J. O. Park and M. Srinivasarao, *Proc. Natl. Acad. Sci.*, 2017, **114**, 3826–3831.
- 44 A. J. Dickinson, N. D. LaRacune, C. B. McKitterick and P. J. Collings, *Mol. Cryst. Liq. Cryst.*, 2009, **509**, 751–762.
- 45 D. M. Agra-Kooijman, G. Singh, A. Lorenz, P. J. Collings, H. S. Kitzerow and S. Kumar, *Phys. Rev. E*, 2014, **89**, 062504–1 – 062504–6.
- 46 V. R. Horowitz, L. A. Janowitz, A. L. Modic, P. A. Heiney and P. J. Collings, *Phys. Rev. E*, 2005, **72**, 041710–1 – 041810–10.
- 47 Y. A. Nastishin, H. Liu, T. Schneider, V. Nazarenko, R. Vasyuta, S. V. Shiyonovskii and O. D. Lavrentovich, *Phys. Rev. E*, 2005, **72**, 041711–1 – 041711–14.



39x39mm (300 x 300 DPI)